JACC Vol. 48, No. 1, 2006
July 4, 2006:176–84

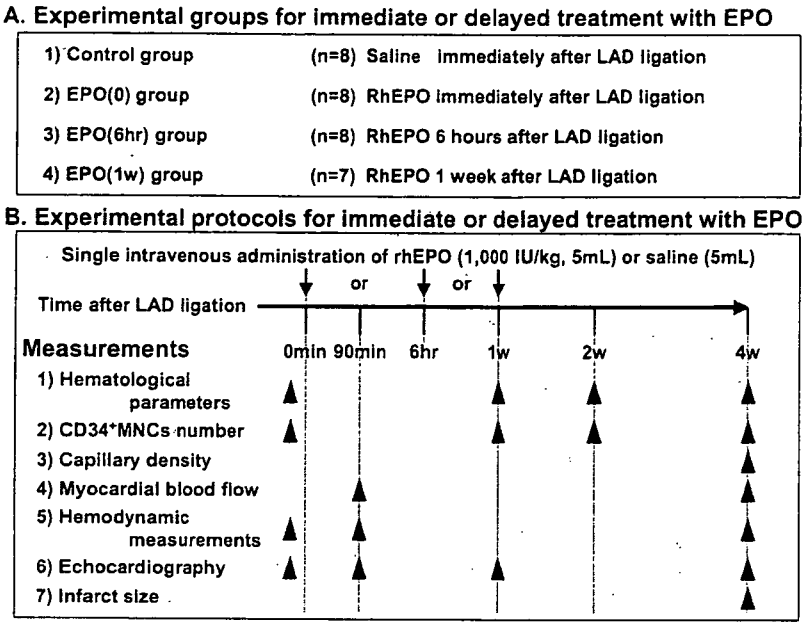

Figure 2. Experimental protocols to investigate effects of immediate or delayed treatment with erythropoietin (EPO) on neovascularization and cardiac function. CD34+MNC = CD34-positive mononuclear cell; other abbreviations as in Figure 1.

MNCs, the number of CD34+MNCs with low cytoplasmic granularity (low sideward scatter) was quantified and expressed as the number of cells per 1-μl blood sample.

In vitro MNC culture assay. Circulating MNCs were isolated from blood (10 ml) of dogs at baseline and 1 week after MI in the control and EPO(0) groups (n = 4 each) by Ficoll density-gradient centrifugation. After MNCs (107 per well) were plated in Medium 199 (Gibco, Grand Island, New York) supplemented with 20% fetal calf serum and antibiotics on human fibronectin-coated six-well dishes. After 7 days in culture, adherent cells were stained for the uptake of 1,1′-dioctadecyl-3,3,3′,3′-tetramethylindocarbocyanine-labeled acetylated low-density lipoprotein (DiI-ac-LDL) (Biomedical Technologies, Stoughton, Massachusetts) and the binding of fluorescein isothiocyanate-labeled *Ulex europaeus* agglutinin I (UEA-I) (Vector Laboratories, Peterborough, England). Double-staining cells were quantified by examining five random microscopic fields (×200 power) (10,11).

Histologic assessments. Four weeks after MI, myocardial tissue was sampled from both ischemic (LAD) and non-ischemic (left circumflex coronary artery [LCX]) regions in each group. The tissues in the ischemic region were identified as the edge of the region showing necrosis. These samples were then fixed in 10% buffered formalin, embedded in paraffin, and serially sectioned in the frontal plane at 5-μm thickness. Endothelial cells were immunohistologically stained using rabbit antihuman von Willebrand factor antibody (Dako, Kyoto, Japan) and the Envision+/HRP Kit (Dako) (17). The peroxidase was visualized by incubation with 3,3'-diaminobenzidine, followed by incubation with a DAB-enhancing solution (Dako). We counted the numbers of capillaries and cardiomyocytes in 20 random high-power fields (×400 power), and then calculated the average capillary density and capillary-to-myocyte ratio (18).

Measurements of regional MBF. Regional MBF was determined as described previously (19). Nonradioactive microspheres (Sekisui Plastic Co., Tokyo, Japan) made of inert plastic were labeled with bromine or niobium. Microspheres were administered at 90 min and 4 weeks after MI. The MBF in the LAD region was calculated according to the following formula: time flow = (tissue count) × (reference flow)/(reference count), and was expressed in ml/g wet weight/min.

Hemodynamic measurements. Hemodynamic parameters, such as arterial mean blood pressure (ABP), heart rate (HR), and left ventricular end-diastolic pressure (LVEDP), were measured at the time points indicated in Figure 2. A 5-F sidearm sheath (Radifocus, Terumo, Tokyo, Japan) was placed in the right femoral artery for hemodynamic measurements. A 4-F pigtail catheter (Outlook, Terumo) was placed in the LV for measurement of LVEDP and was connected to a pressure transducer (model DX-200, Nihon Kohden, Tokyo, Japan). The ABP and HR were monitored via the 5-F sidearm sheath.

Echocardiography. Cardiac function was assessed by echocardiography (Sonos 5500, S4-probe, 2-4 MHz, Philips, Bothell, Washington) at the time points indicated in Figure 2. Short-axis views were recorded at the level of midpapillary muscles, and two-dimensional and M-mode views were recorded at the same level. Measurements of left ventricular end-diastolic dimension (LVEDD) and LV ejection fraction were obtained from M-mode views. All measurements were made by one observer, who was blinded with respect to the identity of the tracings.

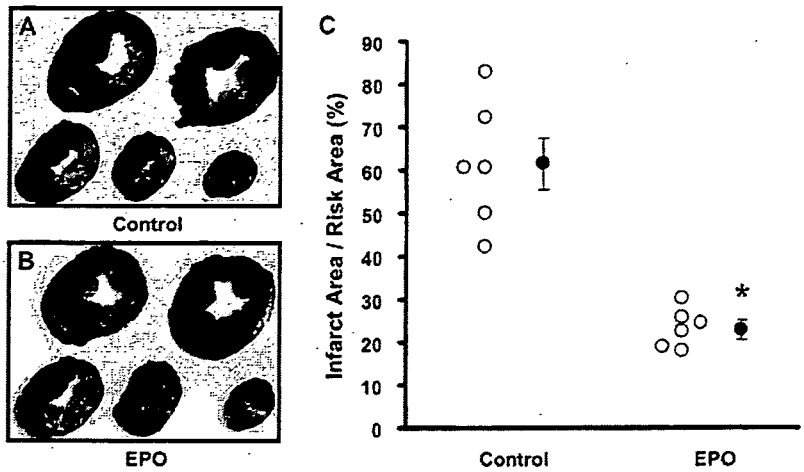

Figure 3. Representative left ventricular cross sections at 6 h after myocardial infarction (MI) in dogs with (**B**) and without (**A**) erythropoietin (EPO) treatment. (**C**) Infarct size at 6 h after MI. *p < 0.05 vs. the control group. **Open circles** = infarct size in each animal.

Infarct size 4 weeks after MI. Myocardial infarct area was determined at the end of the protocol by triphenyltetrazolium chloride staining as described previously (14). Infarct size was expressed as a percentage of the total LV area.

Statistical analysis. Results are expressed as the mean ± standard error of the mean. Comparisons of the time course of the change between groups were performed using two-way repeated measures analysis of variance. Comparisons of other data between groups were performed using one-way factional analysis of variance. If statistical significance was found for a group, a time effect, or a group-by-time interaction, further comparisons were made with paired *t* tests between all possible pairs of four groups at individual time points. The Bonferroni-Holm procedure was used for correction of multiple comparisons. A p value <0.05 was considered to represent statistical significance (20).

RESULTS

Exclusion. Four dogs [acute effects protocol; control: 1, EPO: 0, delayed treatment effects protocol; control: 1, EPO(0): 1, EPO(6h): 0, EPO(1wk): 1] were excluded from analysis because of excessive regional MBF (>15 ml/100 g/min). Thus, 12 and 31 dogs in acute and delayed EPO treatment protocols, respectively, were included.

Acute effects of EPO on infarct size. Myocardial infarct size was significantly smaller in animals receiving EPO compared with those that received saline, but there was no significant difference in regional MBF (9.0 ± 1.0 ml/100 g/min vs. 8.5 ± 1.2 ml/100 g/min) or area at risk (42.9 ± 2.3% vs. 42.3 ± 0.9%) when comparing the two groups (Fig. 3).

Effects of EPO on hematologic parameters. The average change in hematologic parameters was not different when comparing the three EPO-treated groups and the control group over the 4-week experimental protocol (Table 1).

Plasma VEGF levels. Table 2 shows the time course of changes in plasma VEGF level after MI. The plasma VEGF level was significantly and comparably elevated in both control and EPO(0) groups, peaking on 6 h after MI, and returned to baseline at 1 week after MI.

Circulating CD34+MNCs and in vitro cultured MNCs. Figure 4A shows the time course of changes in circulating CD34+MNC number in the different groups. One week after MI, the number of circulating CD34+MNCs increased in all groups. Furthermore, the number of circulating CD34+MNCs at 1 week after MI was higher in the EPO(0) and EPO(6h) groups than in either control or EPO(1wk) group. Two weeks after MI, the number of CD34+MNCs in the control group returned to the baseline. By contrast, the number of CD34+MNCs in the EPO(0) and EPO(6h) groups also decreased but still remained higher than those in either the control or

Table 1. Time Course of Changes in Hematologic Parameters

Parameters	Baseline	1 Week	2 Weeks	4 Weeks
Hematocrit (%)				
Control	52.9 ± 1.7	47.0 ± 1.6	48.9 ± 2.3	53.1 ± 1.8
EPO(0)	52.4 ± 1.1	48.2 ± 1.2	47.9 ± 1.4	53.4 ± 0.7
EPO(6h)	51.5 ± 1.6	49.3 ± 1.6	51.4 ± 1.1	51.3 ± 2.3
EPO(1wk)	48.9 ± 1.0	46.4 ± 1.1	49.4 ± 0.5	50.1 ± 1.0
WBC ($10^3/\mu l$)				
Control	13.8 ± 0.4	15.4 ± 1.4	15.3 ± 0.9	13.5 ± 0.9
EPO(0)	12.6 ± 0.6	14.0 ± 1.1	14.4 ± 0.3	12.3 ± 1.4
EPO(6h)	12.6 ± 0.8	15.6 ± 1.1	13.9 ± 1.0	12.0 ± 0.8
EPO(1wk)	13.1 ± 0.8	14.8 ± 1.2	13.3 ± 0.4	12.9 ± 0.8
Platelet ($10^4/mm^3$)				
Control	27.3 ± 2.0	26.5 ± 1.9	28.4 ± 1.2	26.2 ± 2.0
EPO(0)	28.5 ± 2.0	26.8 ± 4.3	27.0 ± 3.4	28.2 ± 1.8
EPO(6h)	26.9 ± 0.9	27.0 ± 1.4	26.1 ± 1.8	26.1 ± 1.5

Data are presented as mean ± SEM (n = 7 to 8).
EPO = erythropoietin; WBC = white blood cell.

Table 2. Time Course of Changes in Plasma VEGF Levels

Groups	n	Baseline	6 Hours	1 Week	2 Weeks
VEGF (pg/ml)					
Control	4	<9.0	22.5 ± 3.3*	<9.0	<9.0
EPO(0)	4	<9.0	21.6 ± 5.0*	<9.0	<9.0

Data are presented as mean ± SEM. *p < 0.05 vs. baseline.
EPO = erythropoietin; VEGF = vascular endothelial growth factor.

JACC Vol. 48, No. 1, 2006
July 4, 2006:176–84

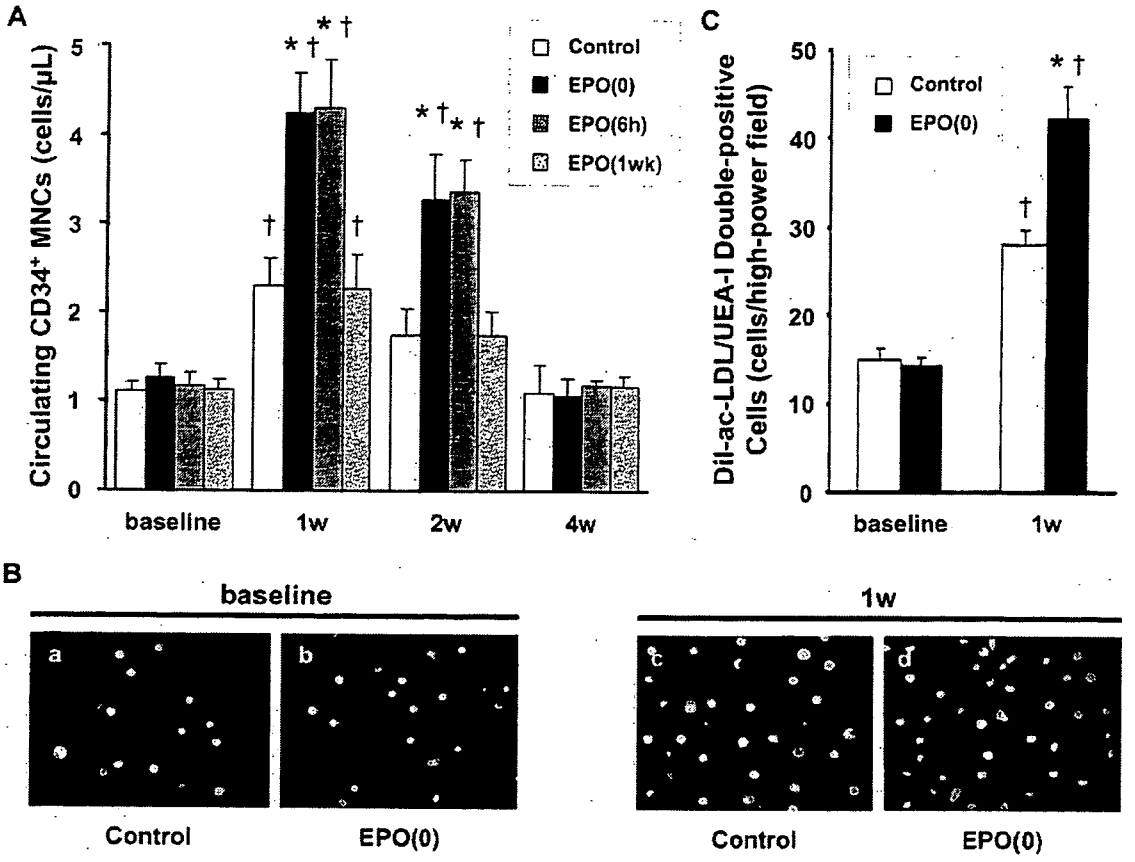

Figure 4. (A) Time course of changes in circulating CD34+MNC count after left anterior descending coronary artery (LAD) ligation in different experimental groups. (B) Representative images of double-stained cultured cells (1,1′-dioctadecyl-3,3,3′,3′-tetramethylindocarbocyanine-labeled acetylated low density lipoprotein [Dil-ac-LDL] and *Ulex europaeus* agglutinin I [UEA-I]) at baseline (a, b) and 1 week after LAD ligation (c, d) from dogs with and without erythropoietin (EPO) treatment immediately after LAD ligation. (C) Quantitative analysis of endothelial progenitor cell culture assay. *$p < 0.05$ vs. the control group. †$p < 0.05$ vs. baseline.

EPO(1wk) group. Furthermore, the administration of EPO 1 week after the LAD ligation did not affect the number of CD34+MNCs at any given time point.

In the culture assay of MNCs, the number of Dil-ac-LDL/UEA-I double-positive cells obtained from blood 1 week after MI increased compared with that at baseline in both control and EPO(0) groups. Importantly, the double-positive cell number obtained from blood 1 week after MI in the EPO(0) group was significantly higher than in the control group (Figs. 4B and 4C).

Capillary density and regional MBF. Figure 5A shows the representative immunohistologic findings in the non-ischemic (panels a to d) and ischemic (panels e to h) regions at 4 weeks after MI. In the nonischemic region, there was no difference in the capillary density and capillary-to-myocyte ratio when comparing groups. In the ischemic region, the capillary-to-myocyte ratio as well as capillary density was significantly higher in the EPO(0) and EPO(6h) groups, but not in the EPO(1wk) group, than in the control group (Figs. 5B to 5C).

Figure 6 shows the changes in regional MBF in the ischemic regions in different experimental groups. There was no significant difference in MBF at 90 min when comparing experimental groups. At 4 weeks after MI, MBF was more increased in the EPO(0) and EPO(6h) groups, but not in the EPO(1wk) group, than in the control group.

Effects of immediate or delayed EPO treatment on cardiac function and infarct size. Throughout the experimental protocols, there was no difference in either ABP or HR when comparing the groups (Table 3).

Figure 7 shows the time course of changes in LVEF (panel A), LVEDD (panel B), and LVEDP (panel C) in different experimental groups. There were no significant differences in baseline LVEF, LVEDD, and LVEDP when comparing the groups.

Ninety minutes, 1 week, and 4 weeks after MI, LVEF was higher in the EPO(0) group than in the other groups. Ninety minutes and 1 week after MI, there was no difference in LVEF when comparing the EPO(6h) group and the control group. When comparing the time points of 1 week and 4 weeks after MI, LVEF decreased in the control and the EPO(1wk) groups but not in the EPO(6h) group. One and 4 weeks after MI, LVEDD was lower in the EPO(0) group than in the other groups. When comparing the time points of 1 week and 4 weeks after MI, LVEDD increased in the control and EPO(1wk) groups but not in the EPO(6h) group. Ninety minutes after MI, LVEDP was lower in the

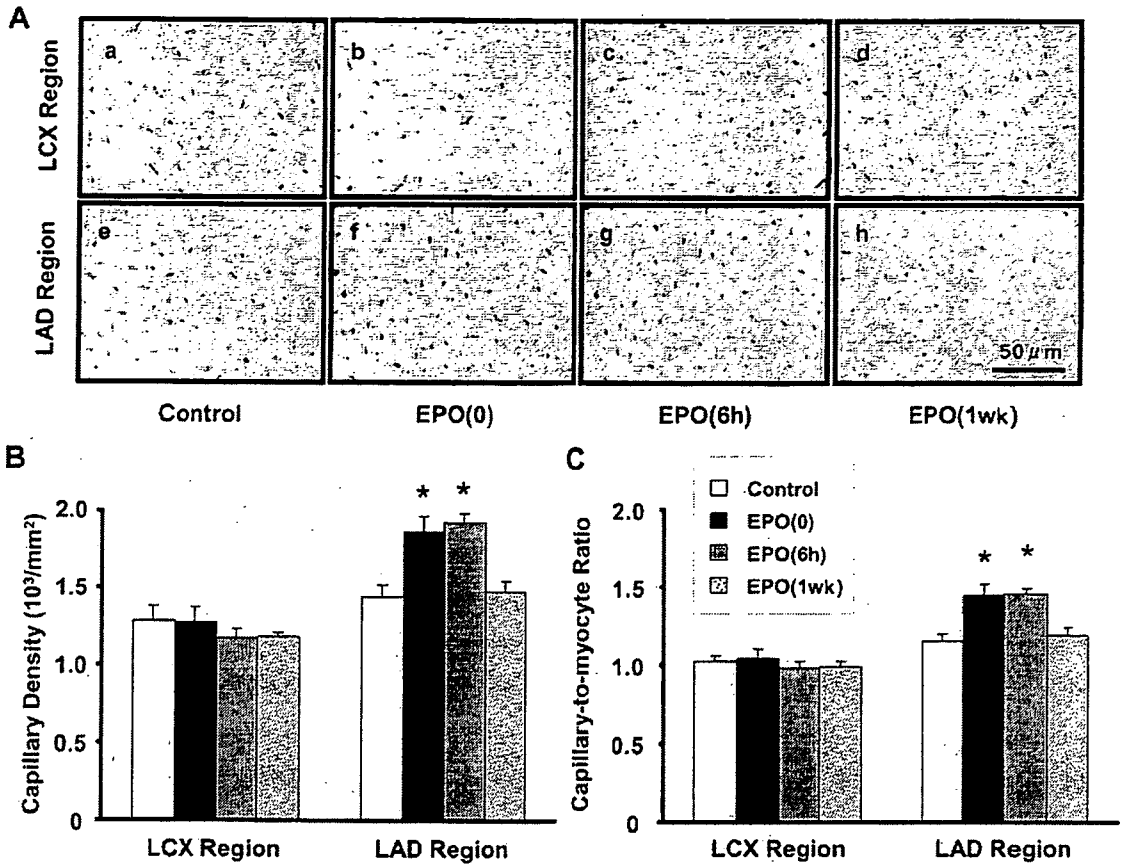

Figure 5. (A) Representative immunohistologic staining with an antibody against von Willebrand factor in nonischemic (left circumflex coronary artery [LCX]) (a, b, c, d) and ischemic (left anterior descending coronary artery [LAD]) (e, f, g, h) regions in different experimental groups. Capillary density (B) and capillary-to-myocyte ratio (C) of nonischemic (LCX) and ischemic (LAD) regions in different experimental groups. *$p < 0.05$ versus the control group. Abbreviations as in Figure 1.

EPO(0) group than in the other groups. Four weeks after MI, LVEDP was lower in the EPO(0) and EPO(6h) groups than in either the control or the EPO(1wk) group.

Myocardial infarct size 4 weeks after MI was smaller in the EPO(0) group than in the control group, although EPO treatment, initiated 6 h and 1 week after MI, did not reduce infarct size (Fig. 7D).

DISCUSSION

The present study showed that EPO administered 6 h after LAD ligation increased circulating CD34+MNCs, capillary density, MBF in the ischemic region, and prevented the worsening of cardiac function without reducing infarct size. The EPO enhances neovascularization, likely via EPC mobilization, and improves cardiac dysfunction in the chronic phase, although EPO has time-window limitations.

We showed that the EPO treatment immediately after the LAD ligation reduced infarct size, which is consistent with observations of previous reports (5–8). Because the infarct size-limiting effects of EPO appear rapidly, the nonerythroid effects of EPO, such as antiapoptosis and radical scavenging (4–8), may contribute to the reduction of infarct size.

Recent reports have shown that circulating CD34+MNC count correlated with EPC number in MNCs culture assay, and both increased at 1 to 2 weeks after EPO administration in animals and humans (9–11). In the culture assay, the number of Dil-ac-LDL/UEA-I double-positive cells obtained from blood at baseline did not differ between the two groups. The number of double-positive cells obtained from blood at 1 week after MI significantly increased compared with that at baseline in the control and EPO(0) groups. Further, the double-positive cell number obtained from blood in the EPO(0) group was higher than in the control group. These findings suggest that EPO augments increases in the number of MNCs that can differentiate into Dil-ac-LDL/UEA-I double-positive cells, an indicator of endothelial cells. Increases in the number of both CD34-positive cells and Dil-ac-LDL/UEA-I double-positive cells strongly suggest that EPO promotes EPC mobilization. The number of CD34+MNCs increased 1 week after MI in the canine model, which is consistent with observations from studies of patients with acute MI (21,22). Furthermore, the number of CD34+MNCs was higher in the EPO(0) and EPO(6h) groups than in the control group. This finding suggests that a single dose of EPO was effective in increasing the number of circulating EPCs after MI. Interestingly,

JACC Vol. 48, No. 1, 2006
July 4, 2006:176–84

EPO administered 1 week after MI failed to produce the identical effect, suggesting that EPO has a time window for promotion of EPC mobilization. We found that plasma VEGF levels were elevated, peaking at 6 h after MI and returned to the baseline 1 week after MI. The EPO did not affect plasma VEGF levels. Because both VEGF and EPO are known to promote EPC mobilization in experimental conditions and are independent predictors for the number of circulating EPCs in patients with coronary heart disease (9–11,23), they may additionally or synergistically contribute to EPC mobilization. Thus, it is likely that EPO alone, at least at the dose used in the present study, might not be enough to promote CD34+MNC mobilization 1 week after MI when VEGF returns to the baseline. Although we only investigated the low dose of EPO to consider the clinical implication, it is possible that high doses of EPO would show the different results. Further investigations are needed to clarify the mechanism of EPO-stimulated EPC mobilization.

The present study also showed that EPO increased capillary-to-myocyte ratio corrected for LV hypertrophy as well as capillary density in the EPO(0) and EPO(6h) groups, suggesting that EPO promotes the neovascularization in the ischemic region. Investigators have also reported that EPO enhances neovascularization in the ischemic region in the hind-limb occlusion model (9). As suggested in the present study, EPO may enhance neovascularization via EPC mobilization. Indeed, bone marrow-derived EPCs incorporate into foci of neovascularization at the border zone of MI (12,13), and administration of ex vivo-expanded EPCs resulted in increased myocardial neovascularization (24,25). In a rat stroke model, Wang et al. (26) showed that EPO treatment, initiated 24 h after MI, enhances angiogenesis. In addition, van der Meer et al. (27) showed that capillary density was increased in the rat post-MI model even when EPO was administered 3 weeks after MI. In contrast, we showed that EPO administered 1 week after MI failed to increase capillary density. The possible explanation for this discrepancy is attributable to the different doses of EPO used. In the studies by Wang et al. (26) (5,000 IU/kg for 7 days) and van der Meer et al. (27) (8,000 IU/kg every 3 weeks), relatively high doses of EPO were administered. In contrast, in the present study, a relatively low dose (1,000 IU/kg) of EPO was administered with a single injection, and the reason for this dose in the present study is for the possible translation of our results to clinical settings more easily (6), because 8,000 or 5,000 IU/kg EPO may cause side effects. On the other hand, we noticed that a higher dose of EPO would increase capillary density and improve the cardiac function even by the late administration of EPO for clinical use.

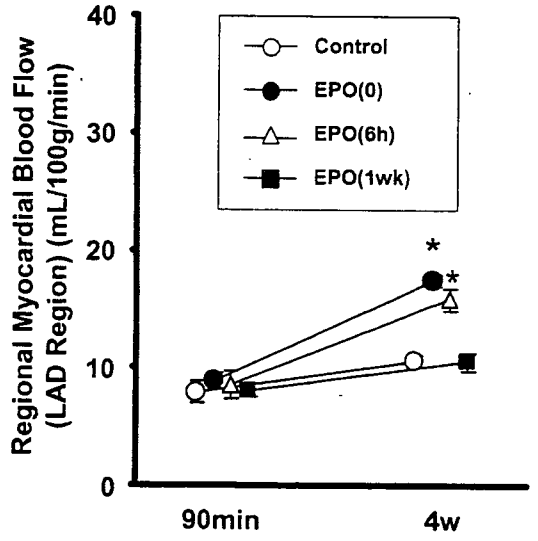

Figure 6. Regional myocardial blood flow in the ischemic (left anterior descending coronary artery [LAD]) region 90 min and 4 weeks after myocardial infarction in different experimental groups. *$p < 0.05$ versus the control group. EPO = erythropoietin.

Table 3. Time Course of Changes in Hemodynamic Parameters

Parameters	Baseline	90 Min	4 Weeks
ABP (mm Hg)			
Control	99 ± 3	101 ± 3	103 ± 2
EPO(0)	102 ± 3	99 ± 3	102 ± 2
EPO(6h)	101 ± 1	98 ± 2	101 ± 1
EPO(1wk)	102 ± 2	102 ± 3	103 ± 2
HR (per min)			
Control	131 ± 6	135 ± 6	129 ± 6
EPO(0)	128 ± 6	131 ± 3	131 ± 5
EPO(6h)	130 ± 7	135 ± 7	126 ± 6
EPO(1wk)	128 ± 6	128 ± 3	126 ± 6

Data are presented as mean ± SEM (n = 7 to 8).
ABP = arterial mean blood pressure; EPO = erythropoietin; HR = heart rate.

In the present study, MBF in the ischemic region was increased in both the EPO(0) and the EPO(6h) groups. Because neovascularization was also enhanced in these groups, increased MBF may occur secondary to the enhanced neovascularization.

The present study also showed that an administration of EPO immediately after the LAD ligation improved cardiac function at 90 min after MI, likely because of infarct size reduction, and subsequently prevented the development of cardiac dysfunction in the chronic phase. Because the previous reports showed that myocardial necrosis progresses within 6 h after the onset of MI (28,29), EPO was administered at time points of 6 h and later after LAD ligation to determine whether its activity is directed toward the acute phase of MI or the chronic phase of cardiac dysfunction. One week after MI, LVEF, LVEDD, or LVEDP was similar among the EPO(6h), EPO(1wk), and control groups. However, EPO administered 6 h, but not 1 week, after the LAD ligation improved cardiac dysfunction 4 weeks after MI when compared with the control group. Because we did not find any difference in infarct size at 4 weeks after MI between the EPO(6h) and the EPO(1wk) groups, the improvement of cardiac function in the EPO(6h) group was not attributable to the reduction of infarct size, but to the increased blood flow to the ischemic regions.

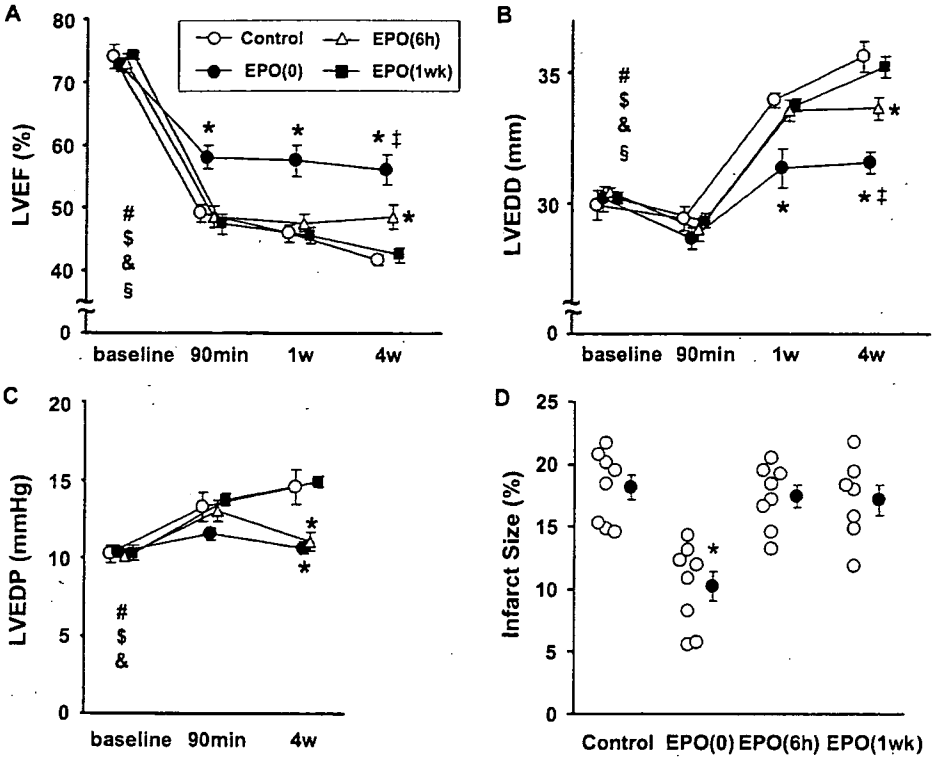

Figure 7. The time course of changes in left ventricular ejection fraction (LVEF) **(A)**, left ventricular end-diastolic dimension (LVEDD) **(B)**, and left ventricular end-diastolic pressure (LVEDP) **(C)** in different experimental groups. Statistically significant ($p < 0.05$) group-by-time interactions (analysis of variance for repeated measurements) are indicated by the following: # = all groups; $ = control × EPO(0) group; & = control × EPO(6h) group; § = EPO(0) × EPO(6h) group. **(D)** Infarct size at 4 weeks after myocardial infarction in different experimental groups. **Open circles** = infarct size in each animal. *$p < 0.05$ versus the control group. EPO = erythropoietin.

In conclusion, in addition to its acute effect on infarct size reduction, EPO may exert chronic cardioprotective effects through neovascularization and may be a useful adjunct for the treatment of patients with myocardial infarction.

Acknowledgments

The authors thank Hiroko Okuda, Akiko Ogai, Yoko Nagamachi, and Nobuko Kawasaki for their technical assistance.

Reprint requests and correspondence: Dr. Tetsuo Minamino, Department of Cardiovascular Medicine, Osaka University Graduate School of Medicine, 2-2 Yamadaoka, Suita, Osaka 565-0871, Japan. E-mail: minamino@medone.med.osaka-u.ac.jp.

REFERENCES

1. Krantz SB. Erythropoietin. Blood 1991;77:419–34.
2. Cotter DJ, Thamer M, Kimmel PL, Sadler JH. Secular trends in recombinant erythropoietin therapy among the U.S. hemodialysis population: 1990–1996. Kidney Int 1998;54:2129–39.
3. Sakanaka M, Wen TC, Matsuda S, et al. In vivo evidence that erythropoietin protects neurons from ischemic damage. Proc Natl Acad Sci U S A 1998;95:4635–40.
4. Chattopadhyay A, Choudhury TD, Bandyopadhyay D, Datta AG. Protective effect of erythropoietin on the oxidative damage of erythrocyte membrane by hydroxyl radical. Biochem Pharmacol 2000;59:419–25.
5. Moon C, Krawczyk M, Ahn D, et al. Erythropoietin reduces myocardial infarction and left ventricular functional decline after coronary artery ligation in rats. Proc Natl Acad Sci U S A 2003;100:11612–7.
6. Hirata A, Minamino T, Asanuma H, et al. Erythropoietin just before reperfusion reduces both lethal arrhythmias and infarct size via the phosphatidylinositol-3 kinase-dependent pathway in canine hearts. Cardiovasc Drugs Ther 2005;19:33–40.
7. Parsa CJ, Matsumoto A, Kim J, et al. A novel protective effect of erythropoietin in the infarcted heart. J Clin Invest 2003;112:999–1007.
8. Lipsic E, van der Meer P, Henning RH, et al. Timing of erythropoietin treatment for cardioprotection in ischemia/reperfusion. J Cardiovasc Pharmacol 2004;44:473–9.
9. Heeschen C, Aicher A, Lehmann R, et al. Erythropoietin is a potent physiologic stimulus for endothelial progenitor cell mobilization. Blood 2003;102:1340–6.
10. Bahlmann FH, DeGroot K, Duckert T, et al. Endothelial progenitor cell proliferation and differentiation is regulated by erythropoietin. Kidney Int 2003;64:1648–52.
11. Bahlmann FH, De Groot K, Spandau JM, et al. Erythropoietin regulates endothelial progenitor cells. Blood 2004;103:921–6.
12. Asahara T, Masuda H, Takahashi T, et al. Bone marrow origin of endothelial progenitor cells responsible for postnatal vasculogenesis in physiological and pathological neovascularization. Circ Res 1999;85:221–8.
13. Asahara T, Murohara T, Sullivan A, et al. Isolation of putative progenitor endothelial cells for angiogenesis. Science 1997;275:964–7.
14. Kitakaze M, Hori M, Morioka T, et al. Alpha 1-adrenoceptor activation mediates the infarct size-limiting effect of ischemic preconditioning through augmentation of 5′-nucleotidase activity. J Clin Invest 1994;93:2197–205.
15. Koumegawa J, Kawahara J, Kubo K, et al. Recombinant human erythropoietin corrects anemia of blood loss: a study in the dog. Int J Cell Cloning 1990;8:97–106.
16. Clifford CA, Hughes D, Beal MW, et al. Plasma vascular endothelial growth factor concentrations in healthy dogs and dogs with hemangiosarcoma. J Vet Intern Med 2001;15:131–5.
17. Horrigan MC, MacIsaac AI, Nicolini FA, et al. Reduction in myocardial infarct size by basic fibroblast growth factor after

JACC Vol. 48, No. 1, 2006
July 4, 2006:176–84

temporary coronary occlusion in a canine model. Circulation 1996;94:1927–33.
18. Pu Q, Larouche I, Schiffrin EL. Effect of dual angiotensin converting enzyme/neutral endopeptidase inhibition, angiotensin converting enzyme inhibition, or AT1 antagonism on coronary microvasculature in spontaneously hypertensive rats. Am J Hypertens 2003;16:931–7.
19. Mori H, Haruyama S, Shinozaki Y, et al. New nonradioactive microspheres and more sensitive x-ray fluorescence to measure regional blood flow. Am J Physiol 1992;263:H1946–57.
20. Holm S. A simple sequentially rejective multiple test procedure. Scand J Stat 1979;6:65–70.
21. Shintani S, Murohara T, Ikeda H, et al. Mobilization of endothelial progenitor cells in patients with acute myocardial infarction. Circulation 2001;103:2776–9.
22. Massa M, Rosti V, Ferrario M, et al. Increased circulating hematopoietic and endothelial progenitor cells in the early phase of acute myocardial infarction. Blood 2005;105:199–206.
23. Asahara T, Takahashi T, Masuda H, et al. VEGF contributes to postnatal neovascularization by mobilizing bone marrow-derived endothelial progenitor cells. Embo J 1999;18:3964–72.
24. Kocher AA, Schuster MD, Szabolcs MJ, et al. Neovascularization of ischemic myocardium by human bone-marrow-derived angioblasts prevents cardiomyocyte apoptosis, reduces remodeling and improves cardiac function. Nat Med 2001;7:430–6.
25. Kawamoto A, Gwon HC, Iwaguro H, et al. Therapeutic potential of ex vivo expanded endothelial progenitor cells for myocardial ischemia. Circulation 2001;103:634–7.
26. Wang L, Zhang Z, Wang Y, Zhang R, Chopp M. Treatment of stroke with erythropoietin enhances neurogenesis and angiogenesis and improves neurological function in rats. Stroke 2004;35:1732–7.
27. van der Meer P, Lipsic E, Henning RH, et al. Erythropoietin induces neovascularization and improves cardiac function in rats with heart failure after myocardial infarction. J Am Coll Cardiol 2005;46:125–33.
28. Reimer KA, Lowe JE, Rasmussen MM, Jennings RB. The wavefront phenomenon of ischemic cell death. 1. Myocardial infarct size vs duration of coronary occlusion in dogs. Circulation 1977;56:786–94.
29. Hirayama A, Adachi T, Asada S, et al. Late reperfusion for acute myocardial infarction limits the dilatation of left ventricle without the reduction of infarct size. Circulation 1993;88:2565–74.

厚生労働科学研究費補助金

医療機器開発推進研究事業

：身体機能解析・補助・代替機器開発研究

逆コンプトン散乱Ｘ線源を用いた医用イメージング法の開発

（H17-ﾌｨｼﾞ-002）

平成17-19年度　総合研究報告書

Vol.2

主任研究者　盛　英三

平成20年（2008年）3月

Available online at www.sciencedirect.com
SCIENCE DIRECT
ELSEVIER
Journal of Pharmacological and Toxicological Methods 53 (2006) 277 – 283
Journal of Pharmacological and Toxicological Methods
www.elsevier.com/locate/jpharmtox

Original article

Long-term monitoring of pulmonary arterial pressure in conscious, unrestrained mice

Daryl O. Schwenke [a,*], James T. Pearson [b], Hidezo Mori [a], Mikiyasu Shirai [c]

[a] *Department of Cardiac Physiology, National Cardiovascular Center Research Institute, 5-7-1 Fujishirodai, Suita, Osaka 565-8565, Japan*
[b] *Department of Physiology, Monash University, Melbourne, Australia*
[c] *Faculty of Health Sciences, Hiroshima International University, Hiroshima, Japan*

Received 10 November 2005; accepted 11 November 2005

Abstract

Introduction: The ability to genetically engineer specific gene 'knock-out' mice has provided a powerful tool for investigating the various mechanisms that contribute to the pathogenesis of pulmonary arterial hypertension (PAH). Yet, so far there have been no reports describing the measurement of pulmonary arterial pressure (PAP) in the conscious wild type mouse—an essential requirement for monitoring dynamic changes associated with the pathogenesis of PAH. Therefore, in this study we describe a new technique for long-term measurement of PAP in conscious unrestrained mice using telemetry. **Methods:** In five male C57BL/6 mice (B.W. 25–30 g), the sensing catheter of a telemetric transmitter was inserted into the right ventricle and advanced into the pulmonary artery. The transmitter body was positioned either within the abdominal cavity or subcutaneously on the back. During recovery from surgery, mean PAP was recorded daily for 1 week. Subsequently, the PAP responses to acute hypoxia (8% O_2 for 10 min) and L-NAME (50 mg/kg, s.c.) were tested in three mice. **Results:** By 1-week post surgery, all mice had fully recovered from surgery and baseline MPAP was stable at 14.9±0.7 mm Hg. Additionally, the pulmonary vascular stimulants acute hypoxia and L-NAME provoked a 63% and 86% increase MPAP, respectively. **Discussion:** In summary, this study has demonstrated the ability to accurately measure PAP by telemetry in conscious, unrestrained mice. One important application of this technique for future studies is the possibility to assess the relative contribution of specific genes (using 'knock-out' mice) during the chronic development of pulmonary pathological conditions.

Keywords: Acute hypoxia; Conscious mouse; L-NAME; Pulmonary arterial pressure

1. Introduction

The mechanisms responsible for the pathogenesis of pulmonary arterial hypertension (PAH) are still not fully understood. In order to investigate potential underlying mechanisms, numerous studies have used pharmacological intervention to selectively block receptor or cellular pathways (e.g. nitric oxide—NO) involved in the modulation of pulmonary vascular tone (Ao, Huang, Zhu, Xiong, & Wang, 2004; Hampl, Archer, Nelson, & Weir, 1993; Hampl, Tristani-Firouzi, Nelson, & Archer, 1996; Huang, Wu, Kang, & Lin, 2002; Weissmann et al., 2001).

In the last decade, the ability to produce targeted gene mutations in the mouse has provided a powerful tool for studying physiological and pathophysiological pathways without pharmacological intervention. Accordingly, various strains of 'knock-out' mice that lack, for example, an isoform of nitric oxide synthase (NOS), have been used for investigating the pathogenesis of PAH (Fagan, Fouty et al., 1990; Fagan, Tyler et al., 1990; Li, Laubach, & Johns, 2001; Quinlan et al., 2000). Thus far, most data have been obtained from in vitro studies, and while such data have aided our understanding of PAH, in vivo studies, in particular using conscious mice, are also essential for investigating the chronic physiological changes within the whole organism, especially during the various developmental stages of PAH.

One of the limiting factors for investigating cardiovascular dynamics in a conscious mouse is its small size. Nevertheless,

* Corresponding author. Tel.: +81 6 6833 5012x2381; fax: +81 6 6835 5416.
E-mail address: schwenke@ri.ncvc.go.jp (D.O. Schwenke).

1056-8719/$ - see front matter © 2005 Elsevier Inc. All rights reserved.
doi:10.1016/j.vascn.2005.11.003

numerous studies have reported the successful use of telemetry for the long-term measurement of systemic arterial pressure in the conscious mouse (Butz & Davisson, 2001; Mills et al., 2000; Tank et al., 2004; Van Vliet, Chafe, & Montani, 2003; Xue, Pamidimukkala, & Hay, 2005).

To date, there is a paucity of literature describing the in vivo measurement of pulmonary arterial pressure (PAP) in the mouse. Several studies have used an anaesthetized preparation, with either a closed- or open-chest model in order to measure PAP in vivo (Champion, Villnave, Tower, Kadowitz, & Hyman, 2000; Steudel et al., 1997; Zhao, Long, Morrell, & Wilkins, 1999). However, the ability to measure pulmonary arterial dynamics in conscious, freely moving mice to, firstly, avoid the depressive effects inherent with the use of anaesthesia and, secondly, to monitor the transient changes in PAP during the development of pathological conditions remains an essential objective in this field of research.

In this study we describe, for the first time, the technique of measuring PAP in the conscious mouse using telemetry. Indwelling catheters have been used for monitoring some cardiovascular variables (e.g. right ventricular pressure) in the conscious mouse (Campen, Shimoda, & O'Donnell, 2005). However, care is required when interpreting data collected using indwelling catheters due to the stress and anxiety associated with the restraint required (Hess, Clozel, & Clozel, 1996). In comparison, the use of telemetry provides more efficient and reliable measurements from freely moving mice (Butz & Davisson, 2001; Mills et al., 2000). Therefore, the protocol we describe in this study uses a commercially available telemetry and data acquisition system to record the systolic, diastolic and mean pulmonary arterial pressure as well as heart rate (HR) of conscious mice.

2. Methods

2.1. Animals

All experiments were approved by the local Animal Ethics Committee and conducted in accordance with the guidelines of the Physiological Society of Japan. Data were collected from five male C57BL/6 mice (~16 weeks old; B.W. 25–30 g). All mice were on a 12-h light/dark cycle at 25±1 °C and were provided with food and water ad libitum.

2.2. Anaesthesia and surgical preparation

All surgical procedures were performed using standard aseptic techniques. Mice were anaesthetized with pentobarbital sodium (60 mg/kg, i.p.) such that the limb withdrawal reflex could not be elicited for the entire surgical period (~90 min). During surgery, body temperature was maintained at 38 °C using a rectal thermistor coupled with a thermostatically controlled heating pad (model BWT-100, BRC Ltd, Tokyo, Japan).

Following anaesthesia induction, the trachea was intubated using a 22-gauge BD Angiocath catheter (Becton Dickinson Inc., Utah, USA) and the lungs were ventilated using a mouse ventilator (Minivent Type 845, Hugo Sachs Elektronik Harvard Apparatus, Germany). The inspirate was enriched with O_2 (~50% O_2) and the ventilator settings were set for a tidal volume of 225 μl and a respiratory frequency of 180 breaths/min.

All surgical areas were shaved and disinfected. The mouse was placed in a supine position and a 2-cm horizontal skin incision was made from the sternum parallel to the 3rd rib on the right side. The right pectoralis major and minor muscles were exposed and retracted. Subsequently, a right thoracotomy was made between the 3rd and 4th rib by blunt dissection.

2.2.1. Positioning of transmitter body

In two mice that had a B.W. of 30 g the body of the telemetric transmitter was placed in the abdominal cavity. The abdomen was opened with a midline abdominal laparotomy and the body of the transmitter was placed into the abdominal cavity. A blunted 21-gauge needle was used as a trocar to pass the transmitter catheter, subcutaneously, from the abdominal incision to the thorax cavity. The abdominal laparotomy was sutured closed.

In the remaining mice (B.W. <30 g), it was considered that the transmitter body would be too big to comfortably fit in the abdominal cavity and, thus, it was positioned subcutaneously on the top of the back. Mice were rolled onto their left side and a dorsal midline incision was made along the back, and the transmitter was placed within the cavity. The transmitter was loosely sutured to the lateral muscles along the back to prevent movement of the transmitter. The transmitter catheter was then passed, subcutaneously, from the back skin incision to the thorax cavity.

With the mouse in a supine position, the 3rd and 4th rib were retracted to expose the right ventricle. A 25-gauge needle was used to gently pierce the conus of the ventricle wall after which the tip of the transmitter catheter (~0.4 mm, thin-walled thermoplastic membrane) was inserted into the right ventricle. Prior to insertion of the catheter, the transmitter was activated (by magnet) and recording of the transmitted signal initiated. Once the catheter was in the ventricle it was slowly advanced anteriorly towards the pulmonary artery until confirmation of its position within the pulmonary artery was evident by monitoring the change in pressure signal. A purse-string tie using 7.0 Prolene suture was used to fix the catheter to the surface of the ventricle wall. The catheter was also externally secured to the 4th and 5th rib for added support. Finally, the thoracotomy was closed with 6.0 silk-thread and all skin incisions were closed with 6.0 Prolene nylon suture.

Immediately following surgery, each mouse received 50 mg/kg (i.m.) of Viccillin® antibiotic (Meiji Seika Kaisha, Ltd, Tokyo Japan) and remained on the heating blanket during recovery from anaesthesia. Mice were gradually weaned off the ventilator when signs of consciousness were evident. However, the weaning time was extended by several hours if any form of sedation/analgesic was administered (i.e. spontaneous breathing was difficult and laboured). Consequently it was elected to avoid sedation during the recovery from anaesthesia. In hindsight, however, it would have been more appropriate to administer a form of analgesia after the mouse had fully

regained consciousness and was back in its housing; a protocol that will be incorporated in future studies. During the subsequent days post-surgery, the welfare of the mouse was monitored by recording body weight, food and water consumption, state of surgical wound healing and observing general appearance and behavior.

2.3. Measurement of heart weight

At the completion of each experiment, each mouse was euthanized by anaesthetic overdose, the heart was excised, the atria were removed, and the right ventricle wall was separated from the left ventricle+septum. Tissues were blotted and weighed. Right and left ventricular weights were expressed as the ratio of the RV to the left ventricular+septum weight ($W_{RV}/W_{LV+septum}$, Fulton's ratio). The heart mass of an additional five mice that underwent sham surgery was also measured. The sham surgery included a thoracotomy, exposing the right ventricle, and a purse-string suture (7.0 Prolene suture) was fixed to the surface of the ventricle wall. The heart mass of sham mice was measured 1 week after surgery.

2.4. Data acquisition by telemetry

Pulmonary arterial pressure (PAP) was measured in the conscious mouse using the telemetry system (Data Sciences, St. Paul, MN, USA). The components of the radio-telemetry system have previously been described in detail (Hess et al., 1996; Mills et al., 2000). The implantable transmitter (model TA11PA-C20) consisted of a catheter (0.4 mm diameter, 40 mm long) and transducer (~12 mm diameter, 23 mm long) and weighed 3.4 g (Data Sciences have subsequently developed a smaller transmitter model (TA11PA-C10) with a weight of only 1.4 g). The tip of the catheter comprised a biocompatible viscous gel that prevented blood reflux and was coated with an anti-thrombogenic film to inhibit thrombus formation. The transmitter signal was relayed from a receiver platform (RPC-1) to a digitized input that was then continuously sampled at 200 Hz with an 8-channel MacLab/8s interface hardware system (AD Instruments Pty Ltd, Japan Inc.), and recorded on a Macintosh Power Book G4 using Chart (v. 5.0.1, AD Instruments). All transmitters were provider pre-calibrated, although the accuracy of the calibrated signal was confirmed using a mercury manometer to within 1.5 mm Hg immediately prior to implantation. Furthermore, during recording the pressure signal from the transmitter was calibrated in reference to atmospheric pressure (Ambient-Pressure Monitor, C11PR). Heart rate (HR) was derived from the pulmonary arterial systolic peaks.

2.5. Experimental protocol

2.5.1. Baseline

Following recovery from anaesthesia, mice were placed in their housing on top of a telemetric receiver. All operated mice were housed with one other non-operated mouse for the entire duration of the study, except for when each operated mouse was tested with hypoxia and/or L-NAME (see below). The PAP of five mice was recorded for 8 consecutive days. The PAP of one mouse was recorded for 14 consecutive days.

2.5.2. Acute hypoxia

The PAP response to acute hypoxia (10 min of 8% O_2) was tested in three mice on either day 7 or day 8 post-surgery. On the day of an experiment, the removable top of the mouse's housing was replaced with a modified lid in order to create a sealed chamber (the non-operated companion mouse had been placed in a separate cage for the day). The air-tight housing was then incorporated in a unidirectional flow circuit into which either air or hypoxia was delivered (~1 L/min). When the inlet gas was switched from air to hypoxia, ~3 min was required to flush the housing with the hypoxic gas. Both air and hypoxia were first humidified before delivery to the housing. The hypoxic gas mixture (i.e. 8% O_2) was produced using gas rotameters (O_2 and N_2). Once the mouse was resting quietly, baseline data were collected for approximately 10 min. Data were continuously recorded as the inlet gas was switched from air to 8% O_2, and then for the duration of hypoxic exposure (10 min) and also during the recovery period. If the mouse became agitated or started moving within its housing, the hypoxic test was terminated and then repeated at a later time.

2.5.3. L-NAME

The three mice that were exposed to hypoxia were also injected with the NO synthase inhibitor, N^{ω}-nitro-L-arginine methyl ester (L-NAME, Sigma-Aldrich, St. Louis, MO., USA) (50 mg/kg, s.c.) either on the same day or 1 day after the hypoxia test. Mice had to be removed from their cage in order to receive the injection; therefore, it was not possible to continuously measure PAP. Furthermore, handling of mice incorporated some degree of stress, so when the mouse was placed back in its cage, it spent 1 to 2 min moving within the cage before starting to relax. Consequently, the effect of L-NAME on PAP could not be accurately measured for approximately 3 min after L-NAME had been injected. Data were continuously recorded for 20 min after L-NAME was injected.

2.6. Data analysis

All data were collected while mice were resting (often sleeping) and relatively inactive. Steady-state data were used for obtaining the mean responses to hypoxia (at the 8th minute of hypoxia) and L-NAME (at the 5th minute after injection) presented in graphs. One-way ANOVA (factorial) was used to test for statistical differences between baseline values and the mean responses for hypoxic and L-NAME. A P-value ≤ 0.05 was predetermined as the level of significance for all statistical analysis.

3. Results

3.1. Recovery from surgery

A total of 15 mice underwent surgery. Three of the mice died during surgery due to factors such as the invasiveness

Fig. 1. A photograph of a normal mouse (right) and a mouse with a telemetric transmitter surgically implanted into its abdominal cavity (left). The transmitter catheter is located within the pulmonary artery for the continuous monitoring of pulmonary arterial pressure (PAP). The PAP traces presented in Fig. 2 were obtained from this mouse. The photo was taken 1 week after surgery.

of the surgery and the potential for excessive blood loss. In the early stages of developing the surgical technique, the primary complication of obtaining PAP from conscious mice, related to the positioning of the catheter tip in an otherwise short (~2 mm) and sharply curved pulmonary arterial trunk. In the first seven mice, the tip of the transmitter catheter was displaced from its original position within the first 2 days post surgery so that the catheter tip was within the ventricle. In such instances it was not possible to measure MPAP, although it was still possible to measure ventricular pressure (which can be used as an estimate of PAP). In subsequent mice, it was elected to secure the transmitter catheter to the 4th and 5th rib to prevent withdrawal of the catheter from the pulmonary artery into the ventricle. This addition to the surgery ensured that pulmonary arterial pressure could be consistently recorded in all remaining mice (i.e. $n=5$).

Although operated mice were comparatively immobile for 2 days after surgery, by the third day mice had started to exhibit normal behavioral patterns for a mouse, such as grooming, burrowing within the housing litter and running around the cage. By day 7, the two mice that had the transmitters positioned in the abdominal cavity were indistinguishable in appearances and activeness from a non-operated mouse, and they had regained body weight to within approximately 1 g of its pre-surgery weight (Fig. 1).

3.2. Baseline PAP

In general, we observed that a clear PAP signal could only be recorded while the mouse was relatively inactive (i.e. resting or sleeping). If the mouse began to run or burrow within its housing, the signal was contaminated by artifacts and therefore illegible. Consequently, it was not possible to continuously obtain a clear PAP signal for 24 h/day. Nevertheless, we were able to record a clear baseline PAP signal in each of the five mice at times of rest for 8 consecutive days after surgery. Typical traces of the recorded PAP signal over the 8-day period are presented in Fig. 2A. Generally, within the first week post-surgery, MPAP fluctuated between 19.9 mm Hg (day 3) and 14.1 mm Hg (day 7) (Fig. 2B). The baseline data obtained from the average of days 7 and 8 post-surgery are presented in Table 1. In one mouse, PAP was recorded for an additional 7 days (total of 14 days), and in this period MPAP remained stable (~16.9 mm Hg by day 14), as it had during the first week post-surgery.

The surgical procedure for pulmonary catheterization caused a small, albeit significant, increase ($P<0.05$) in the RV/LV+septum ratio by 1 week post-surgery (Table 1). The small increase in RV/LV+septum ratio was likely due to the

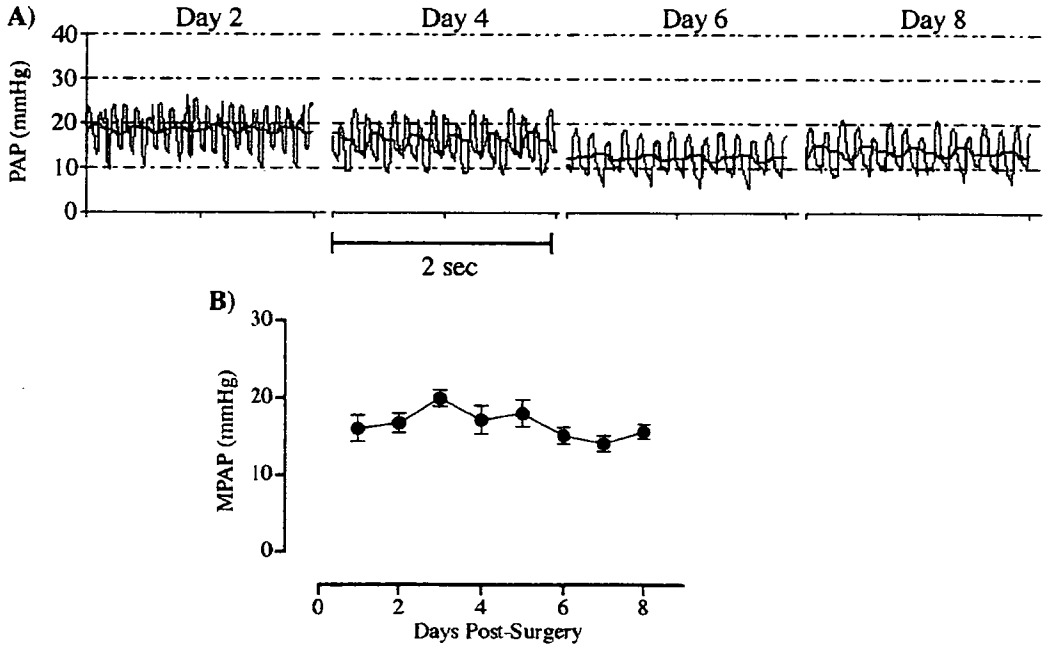

Fig. 2. (A) Example of typical PAP chart traces obtained from a conscious mouse (pictured in Fig. 1) on days 2, 4, 6 and 8 post-surgery. The solid line through the fluctuating PAP trace represents the average PAP. (B) The mean (±S.E.M.) MPAP of five conscious mice recorded each day for 1 week following surgery.

Table 1
Baseline pulmonary arterial pressure and heart mass data of mice

	Transmitter	Sham surgery	No surgery
Mean PAP (mm Hg)	14.9±0.7	N/A	N/A
Systolic PAP (mm Hg)	24±1.2	N/A	N/A
Diastolic PAP (mm Hg)	8.5±0.9	N/A	N/A
HR (bpm)	487±22	N/A	N/A
RV/100 g (mg)	106±5	104±3	94±4
LV+septum/100 g (mg)	278±19	272±11	296±21
RV/LV+septum	0.39±0.01	0.38±0.01	0.32±0.01†

Data are presented as mean±S.E.M. †Significant difference in RV/LV+septum ratio between mice that did not undergo surgery ($n=5$) and operated mice with ($n=5$) or without (sham—$n=5$) a telemetric transmitter (†$P<0.05$).

invasiveness of the surgical procedure (we observed fibrotic tissue surrounding the suture, which was used to anchor the catheter to the wall of the right ventricle), and not due to the presence of a catheter within the pulmonary artery since, (i) sham-operated mice had a similar increase in RV/LV+septum ratio (fibrotic tissue also surrounded the suture) and (ii) there was no increase in baseline pulmonary arterial following the recovery from surgery (an increase in PAP could have increased the workload of the right ventricle provoking right ventricular hypertrophy).

3.3. Pulmonary responses to hypoxia and L-NAME

Three mice were exposed to hypoxia (8% O_2 for 10 min) and, separately, administered L-NAME (50 mg/kg, s.c.) on day 7 or 8 post-surgery. A requisite for collecting data in response to hypoxia and L-NAME was that the mouse remained relatively still in order to obtain a clear PAP signal during data collection. Subsequently, several attempts were made before clear data could be obtained during hypoxia or after L-NAME administration. The mean data are presented in Fig. 3 and a typical transient PAP response to hypoxia and L-NAME recorded in one mouse is illustrated in Fig. 4.

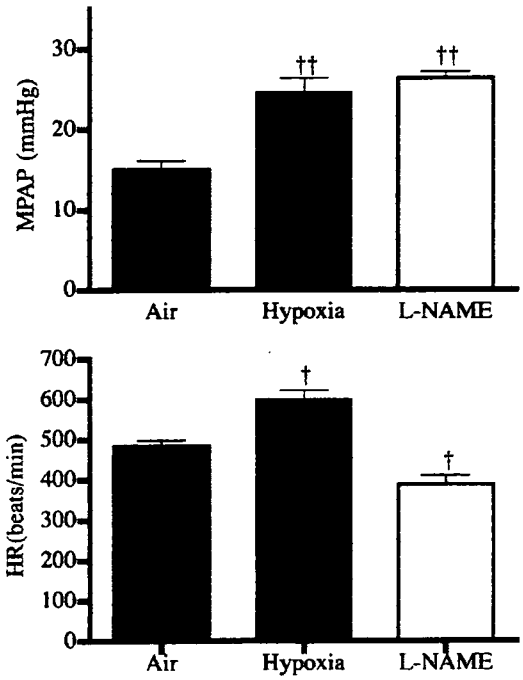

Fig. 3. Steady-state MPAP and HR responses to acute hypoxia (8% O_2 for 10 min) and L-NAME (50 mg/kg, s.c.) in conscious mice. Data ($n=3$) are presented as mean±S.E.M. †Significantly different from baseline (i.e. air) values (†$P<0.01$; ††$P<0.001$).

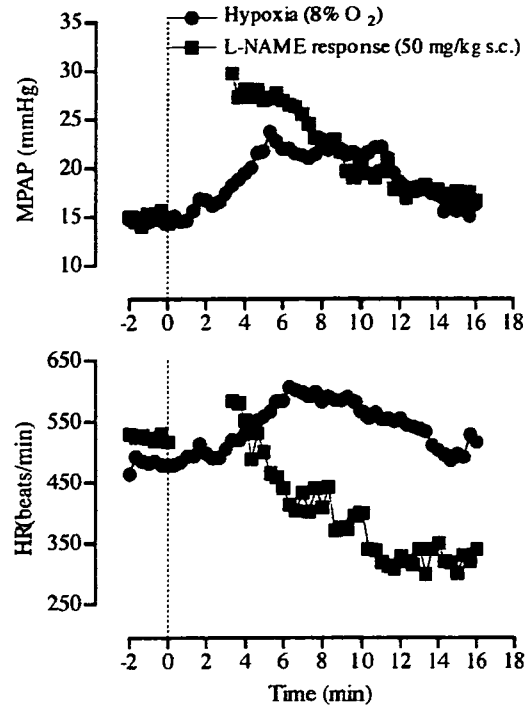

Fig. 4. The transient MPAP and HR responses of a conscious mouse to acute hypoxia (8% O_2 for 10 min) and L-NAME (50 mg/kg, s.c.). Each data point represents the average of a 20-s block of recording. Data could not be recorded while L-NAME was administered, or for the first 3 min after the mouse was placed back into its housing.

During hypoxic exposure MPAP gradually increased before stabilizing ~63% above baseline values ($P<0.001$; Fig. 3), which was sustained until the end of hypoxic exposure. Once the inlet gas was switched back to air, MPAP gradually declined, returning to pre-hypoxia values within approximately 5 min (Fig. 4).

L-NAME (50 mg/kg, s.c.) provoked an 86% increase in MPAP ($P<0.001$; Fig. 3) within 5 min of the injection. Subsequently, MPAP gradually declined back towards pre-L-NAME values (Fig. 4). In general, L-NAME provoked a gradual decline in HR (i.e. baroreflex) that continued for the 20-min period of recording (Fig. 4).

4. Discussion

To the best of our knowledge this is the first study to measure pulmonary arterial pressure (PAP) in the conscious, unrestrained mouse. Furthermore, we were also able to measure the changes in PAP in response to the well-known pulmonary stimulants, hypoxia and L-NAME, effectively demonstrating the reliability of using telemetry for recording a variable range of PAP values in the conscious mouse.

Although no other study has reported the PAP of the conscious mouse, some studies have measured PAP in the anaesthetized mouse and subsequently reported a wide range of MPAP values, depending on whether an open-chest (12.8±1.9 mm Hg, Champion et al., 2000) or closed-chest preparation is used (16.4 to 20.3 mm Hg, Steudel et al., 1997; Zhao et al., 1999). Regardless, the MPAP reported in the conscious mouse of this study (14.9±0.7 mm Hg) is more likely to reflect a 'true' physiological state of the pulmonary vasculature, without the influence of a ventilator or anaesthesia. Campen et al. (2005) monitored right ventricular pressure in conscious mice, but were unable to directly measure PAP.

We monitored MPAP for 8 days after surgery, although we confirmed in one mouse that the PAP signal was stable for 2 weeks and is likely to have remained recordable for considerably longer periods. Indeed, the use of telemetry has previously been validated and shown to provide reliable physiological results (arterial BP) in conscious mice for up to 150 days (Butz & Davisson, 2001; Mills et al., 2000). Therefore, an important advantage arising from this study is the ability to accurately monitor and measure changes in pulmonary vascular modulation during mid-term to long-term studies that involve, for example, pharmaceutical intervention.

The primary limitation of this study is the inability to clearly record MPAP in an over-active mouse. All measurements were taken during the day, when the mouse, a nocturnal rodent, was relatively inactive (e.g. slow walking, eating, resting or sleeping). Therefore data were relatively easy to obtain. However, when attempts were made to collect data overnight, when mice were fully active, the PAP signal often became incomprehensible. This limitation would most likely apply to studies aiming to investigate, for example, pulmonary dynamics during exercise.

There are two main factors that may account for this observed complication. Firstly, it may be due to the presence of a catheter (OD of 0.4 mm) within a very short and sharply curved pulmonary arterial trunk. When the tip was accurately position within the pulmonary artery, any slight forward shift of the catheter (>1.0 mm), such as the mouse running, caused the tip to hit the arterial wall. Secondly, the most likely reason we could not continuously record PAP may be due to signal 'noise' or 'artifacts' generated due to abrupt movement of the transmitter body within the abdomen or on the mouse's back—a common problem observed with the use of telemetry. Recently, Data Sciences developed a considerably smaller transmitter model (TA11PA-C10—weight of 1.4 g) that can fit comfortably within the abdomen of an adult mouse. Therefore, any abrupt movements of the smaller transmitter are less likely to cause illegible noise that is commonly seen when the larger transmitter (i.e. model TA11PA-C20) is placed subcutaneously on the mouse's back.

It has been well documented that both acute hypoxia and the NOS inhibitor L-NAME can cause, via independent mechanisms, vasoconstriction of the pulmonary vasculature, ultimately causing an increase in PAP. The results of our study using the conscious mouse concur with this generally accepted concept. We reported that 8% O_2 induced a 63% increase in MPAP. These results appear more robust than that of the anaesthetized mouse reported by Champion et al. (2000), although their study used a more mild level of hypoxia (~34% increase in MPAP in response to 10% O_2). Similarly, we reported that 50 mg/kg L-NAME (s.c.) provoked an 86% increase in MPAP, which is somewhat larger than that reported for the anaesthetized mouse using the same dose (30% increase in MPAP, Champion et al., 2000). However, Champion et al. (2000) noted that NOS inhibition (using L-NAME) was more effective at provoking vasoconstriction when flow-rate (i.e. cardiac output) was high. Since anaesthesia depresses baseline cardiorespiratory variables and their responses to certain stimulants, the cardiac output of the conscious mouse is likely to be greater than that of the anaesthetized mouse and, therefore, be more susceptible to the inhibition of endothelial NOS by L-NAME. Furthermore, the actual responsiveness of the vasculature to L-NAME is likely to be more robust without the depressive effects of anaesthesia.

In summary, we have demonstrated the ability to measure PAP (including sPAP and dPAP) and HR by telemetry in conscious, unrestrained mice. Despite some limitations of this study, one of the most important advantages is the possibility to monitor and record the transient effects of cardioactive compounds, in normal or genetic 'knockout' mice, without anaesthesia or without the stress that results from more conventional indwelling-catheter techniques.

Acknowledgements

The authors are very grateful for the aid and support provided by the Takeda Science Foundation of Japan.

Conflicts of interest: There is no conflict of interest concerning the material in this manuscript.

References

Ao, Q., Huang, L., Zhu, P., Xiong, M., & Wang, D. (2004). Inhibition of expression of hypoxia-inducible factor-1alpha mRNA by nitric oxide in hypoxic pulmonary hypertension rats. *Journal Huazhong University of Science and Technology Medical Sciences, 24*, 5–8.

Butz, G. M., & Davisson, R. L. (2001). Long-term telemetric measurement of cardiovascular parameters in awake mice: A physiological genomics tool. *Physiological Genomics, 5*, 89–97.

Campen, M. J., Shimoda, L. A., & O'Donnell, C. P. (2005). The acute and chronic cardiovascular effects of intermittent hypoxia in C57BL/6J mice. *Journal of Applied Physiology, 7*.

Champion, H. C., Villnave, D. J., Tower, A., Kadowitz, P. J., & Hyman, A. L. (2000). A novel right-heart catheterization technique for in vivo measurement of vascular responses in lungs of intact mice. *American Journal of Physiology. Heart and Circulatory Physiology, 278*, H8–H15.

Fagan, K. A., Fouty, B. W., Tyler, R. C., Morris, Jr., K. G., Hepler, L. K., Sato, K., et al. (1999). The pulmonary circulation of homozygous or heterozygous eNOS-null mice is hyperresponsive to mild hypoxia. *Journal of Clinical Investigation, 103*, 291–299.

Fagan, K. A., Tyler, R. C., Sato, K., Fouty, B. W., Morris, Jr., K. G., , Huang, P. L., et al. (1999). Relative contributions of endothelial, inducible, and neuronal NOS to tone in the murine pulmonary circulation. *American Journal of Physiology. Lung Cellular and Molecular Physiology, 277*, L472–L478.

Hampl, V., Archer, S. L., Nelson, D. P., & Weir, E. K. (1993). Chronic EDRF inhibition and hypoxia: Effects on pulmonary circulation and systemic blood pressure. *Journal of Applied Physiology, 75*, 1748–1757.

Hampl, V., Tristani-Firouzi, M., Nelson, D. P., & Archer, S. L. (1996). Chronic infusion of nitric oxide in experimental pulmonary hypertension: Pulmonary pressure-flow analysis. *European Respiratory Journal, 9*, 1475–1481.

Hess, P., Clozel, M., & Clozel, J. P. (1996). Telemetry monitoring of pulmonary arterial pressure in freely moving rats. *Journal of Applied Physiology, 81*, 1027–1032.

Huang, K. L., Wu, C. P., Kang, B. H., & Lin, Y. C. (2002). Chronic hypoxia attenuates nitric oxide-dependent hemodynamic responses to acute hypoxia. *Journal of Biomedical Science, 9*, 206–212.

Li, D., Laubach, V. E., & Johns, R. A. (2001). Upregulation of lung soluble guanylate cyclase during chronic hypoxia is prevented by deletion of eNOS. *American Journal of Physiology. Lung Cellular and Molecular Physiology, 281*, L369–L376.

Mills, P. A., Huetteman, D. A., Brockway, B. P., Zwiers, L. M., Gelsema, A. J., Schwartz, R. S., et al. (2000). A new method for measurement of blood pressure, heart rate, and activity in the mouse by radiotelemetry. *Journal of Applied Physiology, 88*, 1537–1544.

Quinlan, T. R., Li, D., Laubach, V. E., Shesely, E. G., Zhou, N., & Johns, R. A. (2000). eNOS-deficient mice show reduced pulmonary vascular proliferation and remodeling to chronic hypoxia. *American Journal of Physiology. Lung Cellular and Molecular Physiology, 279*, L641–L650.

Steudel, W., Ichinose, F., Huang, P. L., Hurford, W. E., Jones, R. C., Bevan, J. A., et al. (1997). Pulmonary vasoconstriction and hypertension in mice with targeted disruption of the endothelial nitric oxide synthase (NOS 3) gene. *Circulation Research, 81*, 34–41.

Tank, J., Jordan, J., Diedrich, A., Obst, M., Plehm, R., Luft, F. C., et al. (2004). Clonidine improves spontaneous baroreflex sensitivity in conscious mice through parasympathetic activation. *Hypertension, 43*, 1042–1047.

Van Vliet, B. N., Chafe, L. L., & Montani, J. P. (2003). Characteristics of 24 h telemetered blood pressure in eNOS-knockout and C57Bl/6J control mice. *Journal of Physiology, 549*, 313–325.

Weissmann, N., Winterhalder, S., Nollen, M., Voswinckel, R., Quanz, K., Ghofrani, H. A., et al. (2001). NO and reactive oxygen species are involved in biphasic hypoxic vasoconstriction of isolated rabbit lungs. *American Journal of Physiology. Lung Cellular and Molecular Physiology, 280*, L638–L645.

Xue, B., Pamidimukkala, J., & Hay, M. (2005). Sex differences in the development of angiotensin II-induced hypertension in conscious mice. *American Journal of Physiology. Heart and Circulatory Physiology, 288*, H2177–H2184.

Zhao, L., Long, L., Morrell, N. W., & Wilkins, M. R. (1999). NPR-A-deficient mice show increased susceptibility to hypoxia-induced pulmonary hypertension. *Circulation, 99*, 605–607.

Biphasic Action of Inducible Nitric Oxide Synthase in a Hindlimb Ischemia Model

Koji Kimura[1], Takako Goto[1], Kentarou Yagi[1], Hidekazu Furuya[1], Shio Jujo[2], Johbu Itoh[3], Sadaaki Sawamura[4], Shirosaku Koide[1], Hidezo Mori[5,*], and Naoto Fukuyama[2,*]

[1]*Department of Surgery, Division of Cardiovascular Surgery, School of Medicine, Tokai University, Kanagawa 259-1193, Japan*
[2]*Department of Physiology School of Medicine, Tokai University, Kanagawa 259-1193, Japan*
[3]*Department of Pathology School of Medicine, Tokai University, Kanagawa 259-1193, Japan*
[4]*Department of Microbiology, School of Medicine, Tokai University, Kanagawa 259-1193, Japan*
[5]*Department of Cardiac Physiology, National Cardiovascular Center, Osaka 565-8565, Japan*

Received 17 October, 2005; Accepted 22 November, 2005

Summary **We investigated the influence of inducible nitric oxide synthase (iNOS) on acute ischemic injury and chronic angiogenesis. In a hindlimb ischemia model, NO produced by endothelial NO synthase (eNOS) reduces ischemic injury and promotes angiogenesis. However, the effect of the large amounts of NO generated by induced iNOS is unclear. Experimental groups of mice were as follows: (1) wild-type group (Wild), (2) iNOS-knockout group (iNOS-KO), and (3) aminoguanidine-treated wild-type group (Wild + AG), which received aminoguanidine from day 0 to day 3 after ischemia. Acute ischemic injury was evaluated by measuring the plasma CK value and ischemic score. Chronic angiogenesis was evaluated by microangiography and with a non-contact type Doppler blood flowmeter on day 3. Compared with the Wild group (251 ± 34.7 IU/l), the CK value was significantly elevated in the iNOS-KO (497 ± 126.7 IU/l) and Wild + AG (587.2 ± 128.7 IU/l) groups. The ischemic score was significantly increased in the iNOS-KO (92%) and Wild ± AG (66.6%) groups compared with the Wild group (23%). Blood flow was significantly increased in the iNOS-KO group (58.7 ± 15.3%) compared with the Wild (38.1 ± 15.9%) and Wild ± AG (43.5 ± 9.8%) groups in the chronic stage. Microangiography revealed a significantly increased number of blood vessels in the iNOS-KO (0.29 ± 0.02) group compared with the Wild (0.12 ± 0.01) and Wild + AG (0.15 ± 0.02) groups. Our findings indicate that NO generated by iNOS has a biphasic action, reducing acute ischemic injury and inhibiting angiogenesis in the chronic stage.**

Key Words: **angiogenesis, ischemia, nitric oxide synthase**

Introduction

The incidence of refractory peripheral arterial disease is increasing rapidly in developed countries [*1*]. When peripheral arterial disease becomes severe, not only is the quality of life of patients impaired, but also their prognosis is poor [*2*]. Consequently new therapies, including angiogenic treatment with vascular endothelial growth factor (VEGF), hepatocyte growth factor (HGF) and fibroblast growth factor-4 (FGF-4) gene transduction or bone marrow cells, have been developed, with some success [*3-8*].

NO is produced by NO synthase and has multiple bioactivities, including vasodilating, anti-platelet-aggregating

*To whom correspondence should be addressed.
Tel: +81-463-931-121 Fax: +81-463-936-684
E-mail: fukuyama@is.icc.u-tokai.ac.jp

and anti-microbial activities [*9*]. Among the three NO synthase isoforms, neuronal NO synthase (nNOS) is found in the central nerve system, and iNOS is induced in smooth-muscle cells and inflammatory cells in various diseases, such as endotoxemia or ischemia, while eNOS is found in vascular endothelial cells [*10*].

NO generally has a cytoprotective action on hindlimb ischemia [*11–14*]. During ischemic injury, eNOS is upregulated and iNOS is induced. It is reasonable that NO produced by eNOS reduces acute ischemic injury and induces angiogenesis, as it has been shown to have a vasodilatory action [*15–17*]. Induced iNOS produces large amounts of NO [*18*], but the effect of NO generated by iNOS in hindlimb ischemia remains unclear.

In this experiment, we examined the contributions of iNOS to the acute phase of ischemic injury and to angiogenesis in the chronic phase of ischemia in a mouse hindlimb ischemia model, using iNOS knockout mice and wild-type mice treated with aminoguanidine (a selective inhibitor of inducible nitric oxide synthese in macrophages)[*19–21*] in the acute phase.

Materials and Methods

Mice

All mice used in experiments were male, 2 to 3 months of age, weighing 18 to 26 g each. Wild-type (Wild) 129 SvEv mice were purchased from CLEA, Japan. iNOS −/− mice, with a mixed C57BL/6J × 129 SvEv genetic background, were obtained from Merck & Co, Inc.. INOS +/+ mice were obtained by crossing 129 SvEv mice with C57BL/6J mice twice. INOS −/− and iNOS +/+ strains have similar genetic backgrounds of 75% C57BL/6J and 25% 129/SvEv [*22*]. For the pharmacologically iNOS-inhibited group, Wild mice were given aminoguanidine (AG; Sigma, 50 mg/kg, i.p., KI value of 55 micro M and a $K_{inact\ max}$ value of 0.09 min^{-1}) [*23*] 24 hr before operation and daily for 3 days postoperatively [*24, 25*]. The animals were maintained in a pathogen-free barrier facility with a 12-hour light/dark cycle and had free access to food and water. Animals were anesthetized with pentobarbital sodium (50 mg/kg, i.p.), and hindlimb ischemia was created by ligation of the left common iliac artery and external iliac artery and resection of the femoral artery [*26, 27*]. Mice were killed 7 days (acute phase) or 14 to 21 days (chronic phase) after surgery [*28*]. The study was approved by the Animal Care Committee of Tokai University.

Evaluation of acute ischemic injury

Serum CK value—To estimate skeletal muscle injury, CK release was estimated in the effluent collected from the infraorbitalis vein on day 3. Plasma was obtained through centrifugation of the whole blood for 10 minutes at 12000 g at 4°C. Plasma was collected and CK was assayed by SRL Co..

Ischemic score—On day 7, the degree of ischemic insult in the limb was macroscopically evaluated by using graded morphological scales for tissue necrosis (grade 0 to IV): grade 0: absence of necrosis: grade I, necrosis only of toes; grade II, necrosis extending to dorsum of a foot; grade III, necrosis extending to crus; grade IV, necrosis extending to a thigh or complete necrosis (Fig. 1).

Evaluation of chronic angiogenesis

Non-contact type laser Doppler measurement—We employed laser Doppler flowmetry (LDF), a non-nvasive technique for measuring tissue blood flow [*16, 29*], using a FLO-N1 device (OMEGAWAVE, Japan), which delivers light generated by a semiconductor laser diode operating at a wavelength of 780 nm, with a maximum accessible power of 3 mW. Briefly, the skin was removed so that only deep muscle blood flow would be measured, and the probe (ST-N probe, OMEGAWAVE, Japan) was placed on 4 points of the femoral muscles. Blood flow was expressed as ml/min/100 g. The contralateral hindlimb served as an internal control.

Sequential microangiography in in vivo—A PE-10 (10-gauge polyethylene) catheter was placed in the right common carotid artery of a mouse fixed on a board (1.0 mm thick) in the standing position under general anesthesia. Sequential images of the hind limb were obtained by the injection of non-ionic contrast material (1 ml/s for 2 s, Iopamidol, Nihon Schering, Tokyo, Japan) via the arterial catheter [*30*] on day 0 and day 14. Monochromatic synchrotron radiation with an energy level of 33.3 keV was obtained with a silicon crystal from beamlines NE5 and BL-14 at the High Energy Accelerator Research Organization, Tsukuba, Japan. To improve contrast resolution, subtraction images were created in the computer from the digital images obtained immediately before and during contrast material injection [*31*]. Angiogenesis was evaluated in terms of vessel density and assigned an angiographic score [*28, 32, 33*]. The ischemic signal in the acute phase is a critical factor inducing angiogenesis [*34*], and angiogenesis increases in proportion to the degree of ischemia [*35, 36*]. Therefore, angiogenesis should be compared among groups with comparable severity of acute ischemic injury. For this reason, we compared results among groups using only animals with grade I ischemic score (refer to Figure 3).

FITC gel angiography—To visualize microvessel networks, the FITC-gelatin conjugate fluorescence injection method (dialyzed FITC, 30 mg/mL conjugated gelatin solution) was employed [*37*]. Mice were anesthetized with pentobarbital sodium (50 mg/kg, i.p.), and a PE-10 (10-gauge polyethylene) catheter was placed in the right common carotid artery. The FITC gelatin solution (20 ml) was injected into the catheter

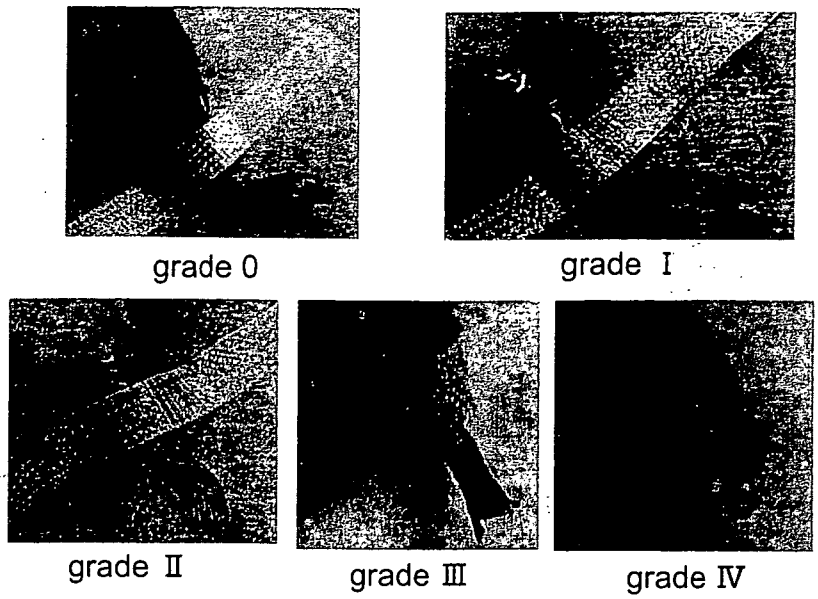

grade	necrotic area
0	none
I	only toes
II	extending to dorsum pedis
III	extending to crus
IV	extending to thigh or complete necrosis

Fig. 1. The grading of necrosis in ischemic hindlimb. The ischemic limb was macroscopically evaluated by using a graded morphological scale for tissue necrosis area (grade 0 to IV).

(1 ml/min) and the right common carotid vein was cut. After complete perfusion, the left leg were resected and immediately fixed in ice-cold graded paraformaldehyde (4%). A confocal laser scanning microscopy (CLSM) system (LSM-410, Carl Zeiss, Jena, Germany), equipped with a 488-nm argon laser (for FITC), was employed on thick sections (1–2 mm) to visualize microvessel networks in detail [*38*]. After computer-assisted 3-D imaging of microvessel networks by the CLSM system, the images were stored on hard disk memory or a magnetic optical disk, EDM-230C (Sony, Tokyo, Japan) and were printed with a digital Pictrostat 400 (Fuji Film Co/Ltd., Tokyo, Japan).

Statistical Analysis

Data are presented as mean values ± SD. Differences were assessed by using one-way ANOVA with Tukey's post test.

Results

Acute ischemic injury

Serum CK value—Firstly, we measured serum CK value to evaluate the acute ischemic injury in the three experimental groups. In the control (Wild) group, the serum CK value was 251 ± 34.7 IU/l. The serum CK values in the Wild + AG group (587.2 ± 128.7 IU/l) and iNOS-KO group (497 ± 126.7 IU/l) were significantly higher than that in the Wild group (Figure 2).

Ischemic score on day 7—The ischemic scores in the iNOS-KO group (92%) and the Wild + AG group (66.6%) were significantly higher than that in the Wild group (23%) (Figure 3). Percentages of grade I in the Wild, iNOS-KO and Wild + AG groups were 23%, 25% and 33%, respectively.

Chronic angiogenesis

Laser Doppler (non contact type) measurement—The

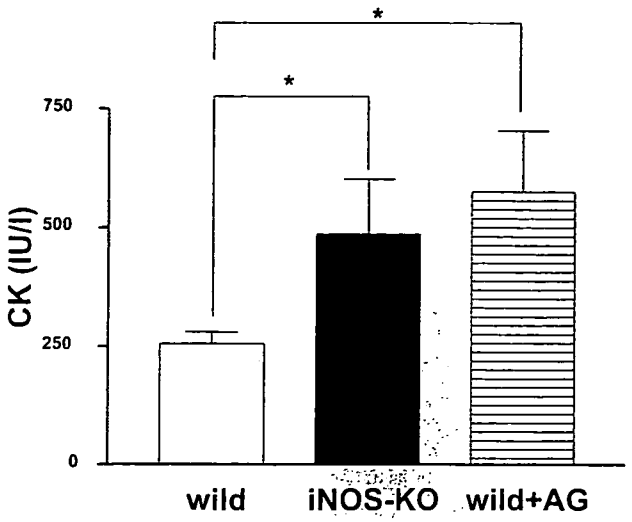

Fig. 2. Serum CK value in acute hindlimb ischemia. Open bar, control group; closed bar, iNOS-knockout (iNOS-KO) group; hatched bar, aminoguanidine-treated group (Wild + AG). The CK values in the iNOS-KO group and Wild + AG group were significantly higher than that in the control (Wild) group (*p<0.05).

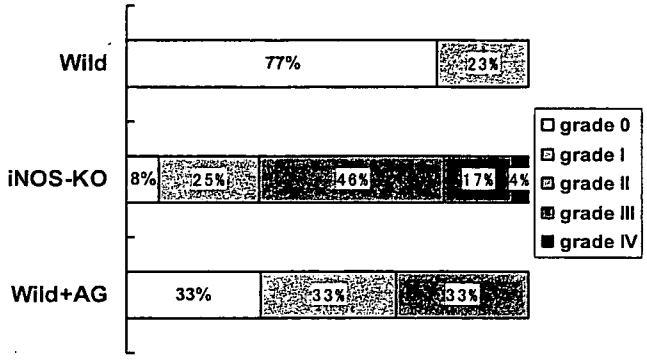

Fig. 3. Ischemic score in acute hindlimb ischemia. Open column, grade 0; dotted column, grade I; vertically lined column, grade II; hatched column, grade III; cross lined column, grade IV.

blood flow at the ischemic lesion was significantly reduced in all three groups on day 3 after surgery. However, at post-operative day 14, it was significantly higher in the iNOS-KO group (58.7 ± 8.7%) than in the Wild group (38.1 ± 5.2%) or the Wild + AG group (43.5 ± 6.4%) (Figure 4).

Sequential microangiography in in vivo—No vessels were apparent in hind limb angiography on day 0, and fine vessels were barely visible on day 14 in the Wild group (Figure 5 A and B). In contrast, many vessels were supplying the hind-limb on the injured side on day 14 in the iNOS-KO group. The angiogenic score on day 14 was significantly increased in the iNOS-KO group (0.29 ± 0.02) compared with that in

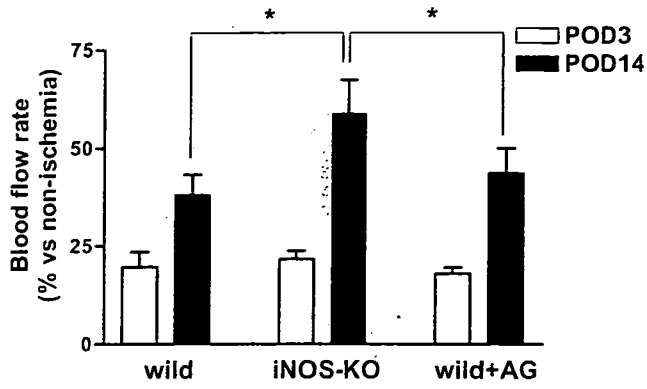

Fig. 4. Blood flow rate in non-contact laser-Doppler flowmetry. Open bar, blood flow ratio on day 3. Closed bar, blood flow ratio on day 14. The blood flow ratio on day 14 in the iNOS-KO group was significantly higher than in the Wild group or Wild + AG group (*p<0.05).

the Wild group or the Wild + AG group (0.12 ± 0.01 and 0.15 ± 0.02, respectively) (p<0.05) (Figure 5).

FITC angiography—The presence of fine vascular networks in the iNOS-KO group (Fig. 6B) implies that marked angiogenesis had occurred. There was a distinct difference in induction of vascular networks between the iNOS-KO group and the Wild and Wild + AG groups (Figure 6 A,B,C).

Discussion

In this experiment, ischemic injury was severe, but angiogenesis was markedly greater in the iNOS-KO group than in the Wild + AG or Wild group. The results indicate that NO generated by iNOS inhibited acute ischemic injury, but reduced angiogenesis in the chronic stage of ischemia.

Of the three NO synthese isoforms, nNOS is mainly localized in the central nervous system, postsynaptic density (PSD), and muscular sarcolemma (muscle fiber myelin) and participates in neural transmission [*39-41*]. iNOS is usually not expressed, but is induced in vascular smooth muscle cells and macrophages *via* cytokine stimulation during sepsis or ischemia with or without reperfusion, and produces large quantities of NO [*42*]. eNOS is mainly localized in vascular endothelial cells and produces NO continuously in response to shear stress, playing important roles in platelet aggregation and vasodilation [*12, 17*]. So, it appears reasonable that NO inhibits acute ischemic injury. In contrast, many studies have shown that NO production by iNOS aggravates injury in the hindlimb ischemia model. Nevertheless, we found that iNOS reduced ischemic injury in the acute stage in the present experiment. A key difference between our study and the others is the presence or absence of reperfusion following the ischemic period. We have

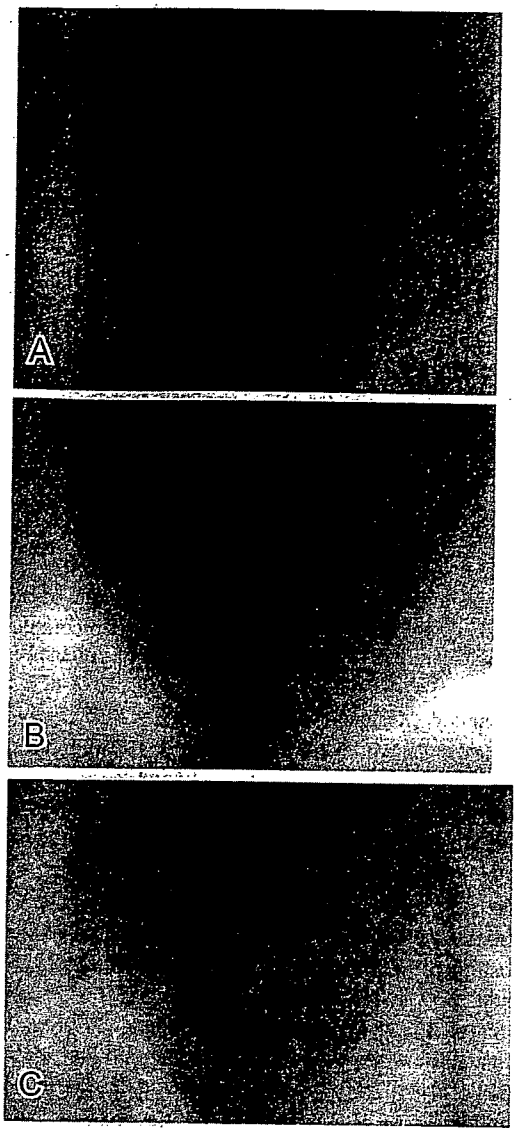

Fig. 5. Representative microangiograms. A : angiogram taken on day 0 in an animal of the Wild group ; B : angiogram taken on day 14 in an animal of the Wild group ; C : angiogram taken on day 14 in an animal of the iNOS-KO group.

already reported that superoxide ($O_2^{\cdot-}$) is produced in ischemic tissue at the time of reperfusion, and reacts with NO to form peroxynitrite [*43*]. Peroxynitrite is a potent oxidant that directly oxidizes sulfhydryl groups at a 1000-fold greater rate than hydrogen peroxide. It inhibits the function of various enzymes, including components of the mitochondrial electron transport chain. In our experiment, we examined ischemia without reperfusion, so that $O_2^{\cdot-}$ (and hence peroxynitrite) would not be produced, and only NO was present.

A second difference from previous experiments is that we used mice treated with iNOS inhibitor in the acute stage, as well as iNOS knockout mice, to examine the effect of iNOS [*44*]. It is noteworthy that one study in which iNOS knockout mice were used and reperfusion was not performed (similar to our protocol) found that injury was severe and angiogenesis in the chronic stage was augmented [*45*]. This is consistent with our results, and indicates that reperfusion plays a critical role in the outcome [*46*].

As the ischemic signal in the acute phase is a critical factor inducing angiogenesis [*34*], and angiogenesis increases in proportion to the degree of ischemia [*35, 36*], angiogenesis has to be compared among groups with comparable severity of acute ischemic injury. We therefore selected animals with grade I ischemic score in all cases for comparison among groups. Aminoguanidine was administered for only three days in the Wild + AG group in order to allow iNOS to function in the chronic stage. At corresponding levels of acute ischemia, angiogenesis in the chronic stage was obviously enhanced in the iNOS-KO group in comparison with the Wild + AG group, i.e., angiogenesis in the chronic stage was inhibited by the function of iNOS.

Many reports indicate that iNOS enhances angiogenesis in various neoplastic disease models [*44, 47–49*]. However, factors secreted by the cancer cells may play important roles in these models. It is important to note that our results showing a biphasic action of iNOS depended on the use of both an acutely iNOS inhibitor-treated wild-type group and an iNOS knockout group in an ischemic model. The mechanism underlying the inhibitory action of NO appears to be down-regulation of the VEGF receptor [*50*]. Possible compensatory roles of eNOS and nNOS in iNOS knockout mice have been ruled out by a previous study, in which their expression was shown to remain unchanged [*51*].

In summary, we have shown that iNOS reduces acute ischemia, but inhibits angiogenesis in a hindlimb ischemia model. Thus we suggest to use iNOS inducer or agents to increase NO production such as arginine with acute phase and supplement iNOS inhibitor in chronic stage. However these remained to be examined prior to clinical trial.

Acknowledgment

This work was supported by grants from Tokai University School of Medicine Research Aid in 2004, the research and study program of Tokai University Educational System General Research Organization and Kanagawa Nanbyou Foundation in 2004, as well as a Grant-in-Aid for Scientific Research in 2003 (No. 15659285) from the Ministry of Education, Science and Culture, Japan and Health and Labour Sciences Research Grants for Research on Human Genome, Tissue Engineering Food Biotechnology in 2003 (H15-saisei-003).